ESAIM: M2AN 51 (2017) 187–207
DOI: 10.1051/m2an/2016011

ESAIM: Mathematical Modelling and Numerical Analysis
www.esaim-m2an.org

A STABILIZED P_1-NONCONFORMING IMMERSED FINITE ELEMENT METHOD FOR THE INTERFACE ELASTICITY PROBLEMS *

Do Y. Kwak[1], Sangwon Jin[1] and Daehyeon Kyeong[1]

Abstract. We develop a new finite element method for solving planar elasticity problems involving heterogeneous materials with a mesh not necessarily aligning with the interface of the materials. This method is based on the 'broken' Crouzeix–Raviart P_1-nonconforming finite element method for elliptic interface problems [D.Y. Kwak, K.T. Wee and K.S. Chang, *SIAM J. Numer. Anal.* **48** (2010) 2117–2134]. To ensure the coercivity of the bilinear form arising from using the nonconforming finite elements, we add stabilizing terms as in the discontinuous Galerkin (DG) method [D.N. Arnold, *SIAM J. Numer. Anal.* **19** (1982) 742–760, D.N. Arnold and F. Brezzi, in *Discontinuous Galerkin Methods. Theory, Computation and Applications*, edited by B. Cockburn, G.E. Karniadakis, and C.-W. Shu. Vol. 11 of *Lecture Notes in Comput. Sci. Engrg.* Springer-Verlag, NewYork (2000) 89–101, M.F. Wheeler, *SIAM J. Numer. Anal.* **15** (1978) 152–161.]. The novelty of our method is that we use meshes independent of the interface, so that the interface may cut through the elements. Instead, we modify the basis functions so that they satisfy the Laplace–Young condition along the interface of each element. We prove optimal H^1 and divergence norm error estimates. Numerical experiments are carried out to demonstrate that our method is optimal for various Lamè parameters μ and λ and locking free as $\lambda \to \infty$.

Mathematics Subject Classification. 65N30, 74S05, 74B05.

Received May 18, 2015. Revised November 19, 2015. Accepted February 1st, 2016.

1. Introduction

Linear elasticity equation plays an important role in solid mechanics. In particular, when an elastic body is occupied by heterogeneous materials having distinct Lamè parameters μ and λ, the governing equation holds on each disjoint domain and certain jump conditions must be satisfied along the interface of two materials [20]. This kind of problems involving composite materials is getting more and more attentions from both engineers and mathematicians in recent years, but efficient numerical schemes are not fully developed yet. To solve such equations numerically, one usually uses finite element methods with meshes aligned with the interface between two materials. However, such methods involve unstructured grids resulting in algebraic systems which involve more unknowns and irregular data structure.

Keywords and phrases. Immersed finite element method, Crouzeix–Raviart finite element, elasticity problems, heterogeneous materials, stability terms, Laplace–Young condition.

* *NRF Grant No. 2014R1A2A1A11053889.*

[1] Department of Mathematical Sciences, Korea Advanced Institute of Science and Technology, Daejeon, Korea.
kdy@kaist.ac.kr; sangwon.jin@gmail.com; huff@kaist.ac.kr

Solving linear elasticity equation with finite element methods has been studied extensively and several methods have been developed (see [2,11,18] and references therein). For lower order methods, when P_1-conforming element method is applied, the so-called 'locking phenomena' is observed when the material is nearly incompressible [4,5,12]. Brenner and Sung [11] showed that the Crouzeix–Raviart (CR) P_1-nonconforming element [17] does not lock on pure displacement problem. But one cannot use this element to a traction-boundary problem since it does not satisfy discrete Korn's inequality. A remedy was recently suggested by Hansbo *et al.* [21] who exploited the idea of discontinuous Galerkin methods [1,3,36]. By introducing a stabilizing term, they proved the convergence of a locking free P_1-nonconforming method for problems with traction boundary conditions.

Solving problems with composite materials is more difficult. Since the Laplace–Young condition holds along the interface, these problems exhibit a similar property as the traction boundary type problems, even if the Dirichlet boundary condition is imposed on the boundary of the whole domain. Thus the CR element may not work properly for such problems. In the discussion of the above methods, meshes are assumed to be aligned with the interface. We will resolve this problem by adding stabilizing terms for unaligned grids (see below).

On the other hand, alternative methods which use meshes independent of interface, thus allowing the interface to cut through the elements, have been developed recently for diffusion problems. The motivations for using such meshes are: Easiness of grid generations, treatment of moving grids, especially time dependent problems, simple data structure of linear system, fast solvers, and so on. There are two types of such methods in principle: One belongs to the extended finite element methods (XFEM) [7,8,22,25,33] and another belongs to the immersed finite element methods (IFEM) [13,14,23,30,31]. In the XFEM type we need, in addition to the standard nodal basis functions, enriched basis functions obtained by truncating the shape functions along the interface cut so that three (six for planar elasticity problems) extra degrees of freedom are present per element. But in the IFEMs, we do not require extra degrees of freedom, instead modify the finite element shape functions so that they satisfy certain jump conditions along the interface.

For some XFEM type of works related to the interface elasticity problems, we refer to [7, 8, 22, 25, 33], where they added enriched basis functions obtained by multiplying Heaviside functions along the crack, and asymptotic basis of polar form near the tip. Even so, they often use grid refinement near the interface. See Hansbo *et al.* [6, 19, 20], where they used Nitsche's [34] idea of adding penalty terms along the interface of elements. For methods based on finite difference, see [24, 27, 28, 35], for example. In the case of IFEM, Lin *et al.* [29] have developed a numerical scheme based on P_1/Q_1 conforming finite elements, but it turns out that P_1/Q_1 conforming IFEM basis functions are not uniquely determined for some range of parameters. So they cannot be used to solve elasticity problems in general. Also, the locking phenomena happens as the Lamé constant λ becomes large. Recently, Lin *et al.* [32] have developed an IFEM based on the rotated Q_1 nonconforming element without using stability terms to solve problems with interface, but no analysis is given.

In this paper, we develop a new method based on the IFEM using the broken CR element for a linear elasticity problem having an interface. We modify the (vector) basis functions to satisfy the Laplace–Young condition along the interface, and add stabilizing terms to ensure the coercivity of the bilinear forms. Our method does not use any extra shape function as in XFEM, hence our method yields exactly the same matrix structure as the problems of constant Lamé parameters, and has less degrees of freedom than XFEM. We proved optimal error estimates of our scheme, in H^1 and L^2 norms. Furthermore, numerical results show that our method does not need a mesh refinement. Regarding to 3D case, we believe a generalization to tetrahedral grids is possible, but showing the existence of basis functions satisfying the Laplace–Young conditions, among others, is more involved. It is left for a future investigation.

The rest of our paper is organized as follows. In Section 2, we introduce the linear elasticity problems having interior interface along which the Laplace–Young condition holds and state their local regularity. For simplicity, we assume the Dirichlet data even though traction boundary condition on some part of boundary can be assigned. In Section 3, we introduce our new scheme for solving such problems using the CR P_1 nonconforming finite element. For this purpose, we modify the vector basis functions so that they satisfy the Laplace–Young condition along the interface. In Section 4, we introduce various norms and function spaces related to interface

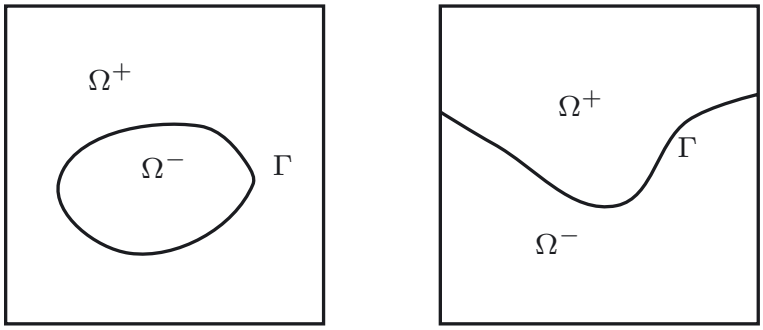

FIGURE 1. Domains Ω with interface.

problems. Next we prove the approximation property of our finite element space and optimal error estimates in H^1 and divergence norm. Finally, numerical experiments are presented in Section 5, which supports our results.

2. Preliminaries

Let Ω be a connected, convex polygonal domain in $\mathbb{R}^2$ which is divided into two subdomains Ω^+ and Ω^- by a C^2 interface $\Gamma = \partial\Omega^+ \cap \partial\Omega^-$, see Figure 1. We assume the subdomains Ω^+ and Ω^- are occupied by two elastic materials having different Lamé constants. For a differentiable function $\mathbf{v} = (v_1, v_2)$ and a tensor $\boldsymbol{\tau} = \begin{pmatrix} \tau_{11} & \tau_{12} \\ \tau_{21} & \tau_{22} \end{pmatrix}$, we let

$$\nabla \mathbf{v} = \begin{pmatrix} \frac{\partial v_1}{\partial x} & \frac{\partial v_1}{\partial y} \\ \frac{\partial v_2}{\partial x} & \frac{\partial v_2}{\partial y} \end{pmatrix}, \ \mathrm{div}\boldsymbol{\tau} = \begin{pmatrix} \frac{\partial \tau_{11}}{\partial x} + \frac{\partial \tau_{12}}{\partial y} \\ \frac{\partial \tau_{21}}{\partial x} + \frac{\partial \tau_{22}}{\partial y} \end{pmatrix}.$$

Then the displacement $\mathbf{u} = (u_1, u_2)$ of the elastic body under an external force satisfies the Navier–Lamé equation as follows.

$$-\mathrm{div}\boldsymbol{\sigma}(\mathbf{u}) = \mathbf{f} \ \text{ in } \Omega^s, \ (s = +, -) \tag{2.1}$$

$$[\mathbf{u}]_\Gamma = 0, \tag{2.2}$$

$$[\boldsymbol{\sigma}(\mathbf{u}) \cdot \mathbf{n}]_\Gamma = 0, \tag{2.3}$$

$$\mathbf{u} = 0 \ \text{ on } \partial\Omega, \tag{2.4}$$

where

$$\boldsymbol{\sigma}(\mathbf{u}) = 2\mu\boldsymbol{\epsilon}(\mathbf{u}) + \lambda tr(\boldsymbol{\epsilon}(\mathbf{u}))\boldsymbol{\delta}, \ \boldsymbol{\epsilon}(\mathbf{u}) = \frac{1}{2}(\nabla\mathbf{u} + \nabla\mathbf{u}^T) \tag{2.5}$$

are the stress tensor and the strain tensor respectively, $\mathbf{n}$ is outward unit normal vector, $\boldsymbol{\delta}$ is the identity tensor, and $\mathbf{f} \in (L^2(\Omega))^2$ is the external force. Here

$$\lambda = \frac{E\nu}{(1+\nu)(1-2\nu)}, \quad \mu = \frac{E}{2(1+\nu)}$$

are the Lamé constants satisfying $0 < \mu_1 < \mu < \mu_2$ and $0 < \lambda < \infty$, E is the Young's modulus, and ν is the Poisson ratio. When the parameter $\lambda \to \infty$, this equation describes the behavior of nearly incompressible material. Since the material properties are different in each region, we set the Lamé constants $\mu = \mu^s, \lambda = \lambda^s$ on Ω^s for $s = +, -$. The bracket $[\cdot]$ means the jump across the interface

$$[\mathbf{u}]_\Gamma := \mathbf{u}|_{\Omega^+} - \mathbf{u}|_{\Omega^-}.$$

Multiplying $\mathbf{v} \in (H_0^1(\Omega))^2$ and applying Green's identity in each domain Ω^s, we obtain

$$\int_{\Omega^s} 2\mu^s \boldsymbol{\epsilon}(\mathbf{u}) : \boldsymbol{\epsilon}(\mathbf{v}) \mathrm{d}x + \int_{\Omega^s} \lambda^s \mathrm{div}\mathbf{u}\, \mathrm{div}\mathbf{v}\, \mathrm{d}x - \int_{\partial\Omega^s} \boldsymbol{\sigma}(\mathbf{u})\mathbf{n} \cdot \mathbf{v} \mathrm{d}s = \int_{\Omega^s} \mathbf{f} \cdot \mathbf{v} \mathrm{d}x, \tag{2.6}$$

where

$$\boldsymbol{\epsilon}(\mathbf{u}) : \boldsymbol{\epsilon}(\mathbf{v}) = \sum_{i,j=1}^{2} \boldsymbol{\epsilon}_{ij}(\mathbf{u}) \boldsymbol{\epsilon}_{ij}(\mathbf{v}).$$

Summing over $s = +, -$ and applying the interior traction condition (2.3), we obtain the following weak form

$$a(\mathbf{u}, \mathbf{v}) = (\mathbf{f}, \mathbf{v}), \tag{2.7}$$

where

$$a(\mathbf{u}, \mathbf{v}) = \int_{\Omega} 2\mu \boldsymbol{\epsilon}(\mathbf{u}) : \boldsymbol{\epsilon}(\mathbf{v}) \mathrm{d}x + \int_{\Omega} \lambda \mathrm{div}\mathbf{u}\, \mathrm{div}\mathbf{v}\, \mathrm{d}x. \tag{2.8}$$

As usual, $(\cdot, \cdot)$ denotes the $L^2(\Omega)$ inner product. Then we have the following result [20, 26].

Theorem 2.1. *There exists a unique solution* $\mathbf{u} \in (H_0^1(\Omega))^2$ *of* (2.1)−(2.4) *satisfying and* $\mathbf{u} \in (H^2(\Omega^s))^2, s = +, -$. *Here,* $H^1(\Omega), H^2(\Omega^s)$ etc., *are usual Sobolev spaces on respective domains and* $H_0^1(\Omega)$ *is a subspace of* $H^1(\Omega)$ *functions having zero trace.*

3. An IFEM based on Crouzeix–Raviart element for the elasticity equation with interface

In this section, we extend the CR type IFEM, which was first suggested by the author [23] for the elliptic problems to the elasticity equation with interface. Before developing the scheme, we briefly review the stabilized version of FEM for the elasticity equation without interface (*i.e.*, $\lambda^+ = \lambda^-$ and $\mu^+ = \mu^-$) introduced by Hansbo and Larson [21].

Let $\{\mathcal{T}_h\}$ be a given quasi-uniform triangulations of Ω by the triangles of maximum diameter h. For each $T \in \mathcal{T}_h$, one constructs local basis functions using the average value along each edge as degrees of freedom. Let

$$\overline{v}|_e = \frac{1}{|e|} \int_e v \mathrm{d}s$$

denote the average of a function $v \in H^1(T)$ along an edge e of T. Here $|S|$ means the Lebesgue measure for any set $S \subset \mathbb{R}^n, n = 1, 2$. Let $\mathbf{N}_h(T)$ denote the linear space spanned by the six Lagrange basis functions

$$\boldsymbol{\phi}_i = (\phi_{i1}, \phi_{i2})^T, \ i = 1, 2, 3, 4, 5, 6$$

satisfying

$$\overline{\phi_{i1}}|_{e_j} = \delta_{i,j}, \quad \overline{\phi_{i2}}|_{e_j} = \delta_{i-3,j}, \quad j = 1, 2, 3,$$

where $\delta_{i,j}$ is the Kronecker delta and sub-index i can take negative integers, *i.e.*, $\delta_{-2,1} = 0, \delta_{-1,2} = 0$ and so on. The vector form of Crouzeix–Raviart P_1-nonconforming space is given by

$$\mathbf{N}_h(\Omega) = \left\{ \begin{array}{c} \boldsymbol{\phi} : \boldsymbol{\phi}|_T \in \mathbf{N}_h(T) \text{ for each } T \in \mathcal{T}_h; \quad \text{if } T_1 \text{ and } T_2 \text{ share an edge } e, \\ \text{then } \displaystyle\int_e \boldsymbol{\phi}|_{\partial T_1} \mathrm{d}s = \int_e \boldsymbol{\phi}|_{\partial T_2} \mathrm{d}s; \text{ and } \int_{\partial T \cap \partial\Omega} \boldsymbol{\phi}\, \mathrm{d}s = \mathbf{0} \end{array} \right\}.$$

The stabilized P_1-nonconforming finite element method for (2.7) is: find $\mathbf{u}_h \in \mathbf{N}_h(\Omega)$ such that

$$a_h(\mathbf{u}_h, \mathbf{v}_h) = (\mathbf{f}, \mathbf{v}_h), \qquad \forall \mathbf{v}_h \in \mathbf{N}_h(\Omega), \tag{3.1}$$

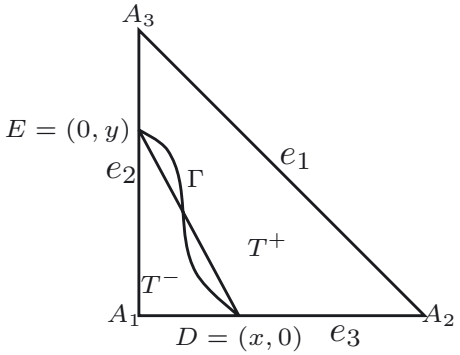

FIGURE 2. A typical interface triangle.

where

$$a_h(\mathbf{u}_h, \mathbf{v}_h) := \sum_{T\in\mathcal{T}_h} \int_T 2\mu\boldsymbol{\epsilon}(\mathbf{u}_h) : \boldsymbol{\epsilon}(\mathbf{v}_h)\mathrm{d}x + \sum_{T\in\mathcal{T}_h} \int_T \lambda \mathrm{div}\mathbf{u}_h \, \mathrm{div}\mathbf{v}_h \, \mathrm{d}x$$
$$+\tau \sum_{e\in\mathcal{E}} \int_e h^{-1}[\mathbf{u}_h][\mathbf{v}_h]\mathrm{d}s \text{ for some } \tau > 0. \tag{3.2}$$

For a problem without an interface, Hansbo and Larson [21] proved the following result.

Theorem 3.1. *Let* $\mathbf{u}$ *be the solution of* (2.1) *and* $\mathbf{u}_h$ *be the solution of* (3.1). *Then*

$$\|\mathbf{u} - \mathbf{u}_h\|_{a_h} \le Ch\|f\|_{L_2(\Omega)},$$

where $\|\cdot\|_{a_h} = a_h(\cdot,\cdot)^{1/2}$.

Construction of broken CR-basis functions satisfying Laplace–Young condition

Now we are ready to introduce our IFEM. We consider an elasticity equation with an interface. Let $\{\mathcal{T}_h\}$ be any quasi-uniform triangulations of Ω of maximum diameter h. We allow the grid to be cut by the interface.

We call an element $T \in \mathcal{T}_h$ an *interface element* if the interface Γ passes through the interior of T, otherwise we call it a *noninterface* element. Let $\mathcal{T}_h^*$ be the collection of all interface elements. We assume the following situations which are easily satisfied when h is small enough:

- the interface intersects the edges of an element at no more than two points.
- the interface intersects each edge at most once, except possibly it passes through two vertices.

The main idea of the IFEM for elasticity problem is to use two pieces of linear shape functions (vector form) on an interface element to satisfy the Laplace–Young condition. We set, for $i = 1, 2, \ldots, 6$,

$$\hat{\boldsymbol{\phi}}_i(x,y) = \begin{cases} \hat{\boldsymbol{\phi}}_i^+(x,y) = \begin{pmatrix} \hat{\phi}_{i1}^+ \\ \hat{\phi}_{i2}^+ \end{pmatrix} = \begin{pmatrix} a_1^+ + b_1^+ x + c_1^+ y \\ a_2^+ + b_2^+ x + c_2^+ y \end{pmatrix}, & (x,y) \in T^+ \\ \hat{\boldsymbol{\phi}}_i^-(x,y) = \begin{pmatrix} \hat{\phi}_{i1}^- \\ \hat{\phi}_{i2}^- \end{pmatrix} = \begin{pmatrix} a_1^- + b_1^- x + c_1^- y \\ a_2^- + b_2^- x + c_2^- y \end{pmatrix}, & (x,y) \in T^- \end{cases} \tag{3.3}$$

and require these functions satisfy the 6 degrees of freedom (edge average), continuity, and jump conditions:

$$\begin{aligned} \overline{\hat{\phi}_{i1}}|e_j &= \delta_{i,j},\ j=1,2,3 \\ \hat{\phi}_{i2}|e_j &= \delta_{i-3,j},\ j=1,2,3 \\ [\hat{\boldsymbol{\phi}}_i(D)] &= 0, \\ [\hat{\boldsymbol{\phi}}_i(E)] &= 0, \\ \left[\boldsymbol{\sigma}(\hat{\boldsymbol{\phi}}_i)\cdot\mathbf{n}\right]_{\overline{DE}} &= 0, \end{aligned} \tag{3.4}$$

These twelve conditions lead to a system of linear equations in twelve unknowns for each i.

Proposition 3.2. *The conditions* (3.4) *uniquely determine the function* $\hat{\boldsymbol{\phi}}_i$ *of the form* (3.3)*, regardless of the interface locations.*

Proof. See Appendix for details. □

We denote by $\widehat{\mathbf{N}}_h(T)$ the space of functions generated by $\hat{\boldsymbol{\phi}}_i, i=1,2,3,4,5,6$ constructed above. Using this local finite element space, we define the global *immersed finite element space* $\widehat{\mathbf{N}}_h(\Omega)$ by

$$\widehat{\mathbf{N}}_h(\Omega) = \left\{ \begin{array}{l} \hat{\boldsymbol{\phi}} \in \widehat{\mathbf{N}}_h(T) \text{ if } T \in \mathcal{T}_h^*, \text{ and } \hat{\boldsymbol{\phi}} \in \mathbf{N}_h(T) \text{ if } T \notin \mathcal{T}_h^*; \\ \text{ if } T_1 \text{ and } T_2 \text{ share an edge } e, \text{ then} \\ \int_e \hat{\boldsymbol{\phi}}|_{\partial T_1}\mathrm{d}s = \int_e \hat{\boldsymbol{\phi}}|_{\partial T_2}\mathrm{d}s; \text{ and } \int_{\partial T\cap\partial\Omega} \hat{\boldsymbol{\phi}}\,\mathrm{d}s = \mathbf{0} \end{array} \right\}.$$

We now propose an IFEM scheme for (2.1)–(2.4).

CRIFEM

Find $\mathbf{u}_h \in \widehat{\mathbf{N}}_h(\Omega)$ such that

$$a_h(\mathbf{u}_h, \mathbf{v}_h) = (\mathbf{f}, \mathbf{v}_h), \quad \forall \mathbf{v}_h \in \widehat{\mathbf{N}}_h(\Omega), \tag{3.5}$$

where $a_h(\cdot,\cdot)$ is the same as (3.2).

4. Error analysis

We introduce function spaces and norms that are necessary for analysis. Let $p \geq 1$ and $m \geq 0$ be an integer. For any domain D, we let $W_p^m(D)$ ($H^m(D) = W_2^m(D)$) be the usual Sobolev space with (semi)-norms denoted by $|\cdot|_{m,p,D}$ and $\|\cdot\|_{m,p,D}$. ($\|\cdot\|_{m,D} = \|\cdot\|_{m,2,D}$). For $m=1,2$ and any domain $D = T(\in \mathcal{T}_h)$ or $D=\Omega$, let

$$(\widetilde{W}_p^m(D))^2 := \{\mathbf{u} = (u_1,u_2) \in (W_p^{m-1}(D))^2 :\ u|_{D\cap\Omega^s} \in (W_p^m(D\cap\Omega^s))^2, s = +,-\}$$

with norms

$$|\mathbf{u}|^p_{\widetilde{W}^m(D)} := |\mathbf{u}|^p_{m,p,D\cap\Omega^+} + |\mathbf{u}|^p_{m,p,D\cap\Omega^-}, \quad \text{and } \|\mathbf{u}\|^p_{\widetilde{W}^m(D)} := \|u\|^p_{m-1,p,D} + |\mathbf{u}|^p_{\widetilde{W}^m(D)}.$$

When $p=2$, we write $(\widetilde{H}^m(D))^2 := (\widetilde{W}_p^m(D))^2$ and denote the norms (resp. semi norms) by $\|\mathbf{u}\|_{\widetilde{H}^m(D)}$ (resp. $|\mathbf{u}|_{\widetilde{H}^m(D)}$), *etc.* When a finite element triangulation $\{\mathcal{T}_h\}$ is involved, the norms are understood as piecewise norms $(\sum_{T\in\mathcal{T}_h} \|\mathbf{u}\|^p_{\widetilde{W}_p^m(T)})^{1/p}$, *etc.* If $p=2$, we denote them by $\|\mathbf{u}\|_{m,h}$ (resp. $|\mathbf{u}|_{m,h}$). Let $\mathbf{H}_h(\Omega) := (H_0^1(\Omega))^2 + \widehat{\mathbf{N}}_h(\Omega)$. We need subspaces of $(\widetilde{H}^2(T))^2$ and $(\widetilde{H}^2(\Omega))^2$ satisfying the jump conditions:

$$\begin{aligned} (\widetilde{H}^2_I(T))^2 &:= \{\mathbf{u} \in (\widetilde{H}^2(T))^2 \text{ and } [\boldsymbol{\sigma}(\mathbf{u})\cdot\mathbf{n}]_{\Gamma\cap T} = 0\}, \\ (\widetilde{H}^2_I(\Omega))^2 &:= \{\mathbf{u} \in (H_0^1(\Omega))^2\ \mathbf{u}|_T \in (\widetilde{H}^2_I(T))^2,\ \forall T \in \mathcal{T}_h\}. \end{aligned}$$

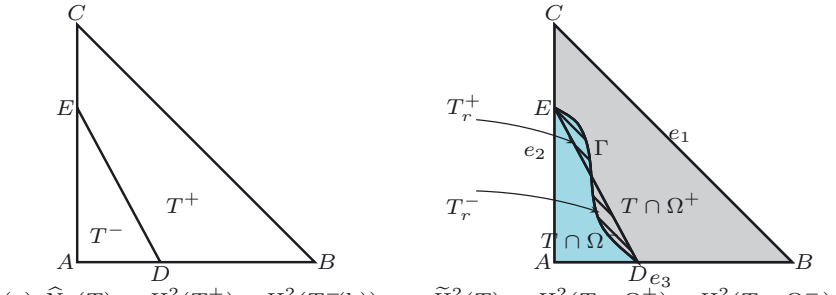

(a) $\widehat{N}_h(T) \subset H^2(T^+) \cap H^2(T^-$(b)) $\widetilde{H}^2(T) \subset H^2(T \cap \Omega^+) \cap H^2(T \cap \Omega^-)$

FIGURE 3. The real interface and the approximated interface.

Throughout the paper, the constants C, C_0, C_1, *etc.*, are generic constants independent of the mesh size h and functions $\mathbf{u}, \mathbf{v}$ but may depend on the problem data $\mu, \lambda, \mathbf{f}$ and Ω, and are not necessarily the same on each occurrence.

To prove the H^1-error estimates it suffices to estimate 'the approximation error' and 'the consistency error'. The details are given in Theorem 4.9 in Section 4.2.

4.1. Approximation property of $\widehat{\mathbf{N}}_h(T)$

Note that the case of a scalar elliptic problem is given in [23]. One of the obstacles in proving the approximation property is: the space $\widehat{\mathbf{N}}_h(T)$ does not belong to $(\widetilde{H}^2_\Gamma(T))^2$ because the curved interface is approximated by the line segment. To overcome this difficulty, we introduce a bigger space which contains both of these spaces. For a given interface element T, we define function spaces $X(T)$ and $X_\Gamma(T)$ by

$$X(T) := \left\{\mathbf{u} : \mathbf{u} \in (H^1(T))^2, \mathbf{u} \in (H^2(S))^2 \text{ for all } S = T_r^+, T_r^-, T^+ \cap \Omega^+, T^- \cap \Omega^-\right\} \tag{4.1}$$

$$X_\Gamma(T) := \left\{\mathbf{u} : \mathbf{u} \in X(T), \int_{\Gamma \cap T} (\boldsymbol{\sigma}(\mathbf{u})^- - \boldsymbol{\sigma}(\mathbf{u})^+) \cdot \mathbf{n}_\Gamma \, \mathrm{d}s = 0\right\} \tag{4.2}$$

where $\boldsymbol{\sigma}(\mathbf{u})^- = 2\mu^- \boldsymbol{\epsilon}(\mathbf{u}) + \lambda^- \mathrm{div}\mathbf{u}$, $\boldsymbol{\sigma}(\mathbf{u})^+ = 2\mu^+ \boldsymbol{\epsilon}(\mathbf{u}) + \lambda^+ \mathrm{div}\mathbf{u}$ and $S = T_r^+, T_r^-, T^+ \cap \Omega^+, T^- \cap \Omega^-$ are subregions of T created by Γ and line segment $\overline{DE}$ (see Fig. 3).

Note the relations

$$(\widetilde{H}^2(T))^2 \hookrightarrow X(T) \hookrightarrow (H^1(T))^2 \tag{4.3}$$

$$(\widetilde{H}^2_\Gamma(T))^2 \cup \widehat{\mathbf{N}}_h(T) \hookrightarrow X_\Gamma(T) \hookrightarrow X(T) \hookrightarrow (H^1(T))^2 \tag{4.4}$$

For any $\mathbf{u} \in X(T)$, we define the following norms:

$$\begin{aligned}
\|\mathbf{u}\|^2_{b,m,T} &= \|\mathbf{u}\|^2_{m,T} + m \cdot \|\sqrt{\lambda}\mathrm{div}\mathbf{u}\|^2_{0,T},\ m = 0, 1\\
|\mathbf{u}|^2_{X(T)} &= |\mathbf{u}|^2_{2,T^- \cap \Omega^-} + |\mathbf{u}|^2_{2,T^+ \cap \Omega^+} + |\mathbf{u}|^2_{2,T_r^-} + |\mathbf{u}|^2_{2,T_r^+},\\
\|\mathbf{u}\|^2_{X(T)} &= \|\mathbf{u}\|^2_{1,T} + |\mathbf{u}|^2_{X(T)} + \|\sqrt{\lambda}\mathrm{div}\mathbf{u}\|^2_{0,T} + \sum_{s=+,-} |\sqrt{\lambda}\mathrm{div}\mathbf{u}|^2_{1,T^s}\\
|\!|\!|\mathbf{u}|\!|\!|^2_{2,T} &= |\mathbf{u}|^2_{X(T)} + \sum_{s=+,-} |\sqrt{\lambda}\mathrm{div}\mathbf{u}|^2_{1,T^s}\\
&\quad + \left|\int_{\Gamma \cap T} [\boldsymbol{\sigma}(\mathbf{u})\mathbf{n}_\Gamma] \, \mathrm{d}s\right|^2 + \sum_{i=1}^{3} |\overline{u_1}|_{e_i}|^2 + \sum_{i=1}^{3} |\overline{u_2}|_{e_i}|^2.
\end{aligned}$$

Note that when $m = 0$, $\|\mathbf{u}\|^2_{b,m,T}$ is just the L^2-norm $\|\mathbf{u}\|^2_{0,T}$. For $\mathbf{v} \in \mathbf{H}_h(\Omega)$, define

$$\|\mathbf{v}\|^2_{a_h} := a_h(\mathbf{v},\mathbf{v}) = \sum_{T\in\mathcal{T}_h}\left(\int_T 2\mu\epsilon(\mathbf{v}) : \epsilon(\mathbf{v})\mathrm{d}x + \int_T \lambda|\mathrm{div}\mathbf{v}|^2\mathrm{d}x\right) + \sum_{e\in\mathcal{E}}\int_e \frac{\tau}{h}[\mathbf{v}]^2\mathrm{d}s. \tag{4.5}$$

Remark 4.1.

(1) The difference between the spaces $(\widetilde{H}^2(T))^2$ and $X(T)$ is this: a function $\mathbf{u} \in (\widetilde{H}^2(T))^2$ is H^2 in each of the regions T^+ and T^- while a function $\mathbf{u} \in X(T)$ is H^2 in each of the four regions $T_r^+, T_r^-, T^+\cap\Omega^+, T^-\cap\Omega^-$.
(2) The difference between the spaces $(\widetilde{H}^2_\Gamma(T))^2$ and $X_\Gamma(T)$ is this: a function $\mathbf{u} \in (\widetilde{H}^2_\Gamma(T))^2$ satisfies the a strong Laplace–Young condition (2.3) along Γ while $\mathbf{u} \in X_\Gamma(T)$ satisfies it weakly: $\int_{\Gamma\cap T}(\boldsymbol{\sigma}(\mathbf{u})^- - \boldsymbol{\sigma}(\mathbf{u})^+)\cdot\mathbf{n}_\Gamma\,\mathrm{d}s = 0$. In fact, for every continuous, piecewise linear functions, this condition holds if and only if it satisfies the same condition along the line segment joining the end points of the interface, as shown in the Lemma below.

Lemma 4.2. *For an interface triangle T, every continuous, piecewise linear function $\boldsymbol{\phi}$ satisfies*

$$\int_{\Gamma\cap T}[\boldsymbol{\sigma}(\boldsymbol{\phi})\cdot\mathbf{n}_\Gamma]\mathrm{d}s = 0 \text{ if and only if } \int_{\overline{DE}}[\boldsymbol{\sigma}(\boldsymbol{\phi})\cdot\mathbf{n}_{\overline{DE}}]\mathrm{d}s = 0. \tag{4.6}$$

Proof. This can be easily proved by Green's theorem since $\boldsymbol{\phi}$ is piecewise linear. □

Lemma 4.3. $\|\!|\cdot|\!\|_{2,T}$ *is a norm on the space $X_\Gamma(T)$ which is equivalent to $\|\cdot\|_{X(T)}$.*

Proof. Clearly, $\|\!|\cdot|\!\|_{2,T}$ is a semi-norm. To show it is indeed a norm, assume $\mathbf{u} \in X_\Gamma(T)$ satisfies $\|\!|\mathbf{u}|\!\|_{2,T} = 0$. Then $|\mathbf{u}|_{X(T)} = 0$. Hence $\mathbf{u}$ is linear on each of the four regions $T^+\cap\Omega^+$, $T^-\cap\Omega^-$, T_r^+ and T_r^-. Since $\mathbf{u} \in H^1(T)$, $\mathbf{u}$ is continuous on T. Since $\int_{\Gamma\cap T}[\boldsymbol{\sigma}(\mathbf{u})\cdot\mathbf{n}_\Gamma]\,\mathrm{d}s = 0$, $\mathbf{u}$ satisfies the interface condition along the line segment $\overline{DE}$ by Lemma 4.2. Hence $\mathbf{u} \in \widehat{\mathbf{N}}_h(T)$ and together with the fact that $\overline{u_1}_{e_i} = 0,\ i = 1,2,3$ and $\overline{u_2}_{e_i} = 0,\ i = 1,2,3$, we conclude $\mathbf{u} = 0$, which shows that $\|\!|\cdot|\!\|_{2,T}$ is a norm.

We now show the equivalence of $\|\!|\cdot|\!\|_{2,T}$ and $\|\cdot\|_{X(T)}$ on the space $X_\Gamma(T)$. (*cf.* [9], p. 77). By Sobolev embedding,

$$\sum_{i=1}^3|\overline{u_1}_{e_i}| + \sum_{i=1}^3|\overline{u_2}_{e_i}| \le C\max_{s=+,-}\|\mathbf{u}\|_{L^\infty(T^s)} \tag{4.7}$$

$$\le C\max_{s=+,-}\|\mathbf{u}\|_{H^2(T^s)} \le C\|\mathbf{u}\|_{\widetilde{H}^2(T)}. \tag{4.8}$$

$$\le C\|\mathbf{u}\|_{X(T)}. \tag{4.9}$$

Hence we see

$$\|\!|\mathbf{u}|\!\|_{2,T} \le C\|\mathbf{u}\|_{X(T)}. \tag{4.10}$$

Now suppose that the converse

$$\|\mathbf{u}\|_{X(T)} \le C\|\!|\mathbf{u}|\!\|_{2,T}, \quad \forall\mathbf{u} \in X_\Gamma(T)$$

fails for any $C > 0$. Then there exists a sequence $\{\mathbf{u}_k\}$ in $X_\Gamma(T)$ with

$$\|\mathbf{u}_k\|_{X(T)} = 1, \quad \|\!|\mathbf{u}_k|\!\|_{2,T} \le \frac{1}{k}, \quad k = 1,2,\ldots \tag{4.11}$$

Let $S_t, t = 1,\ldots,4$ denote the four subregions defined in the definition of $X(T)$. Since $H^2(S_1)$ is compactly embedded in $H^1(S_1)$, ([15], p. 114), there exists a subsequence of $\{\mathbf{u}_k\}$ which converges in $(H^1(S_1))^2$. Applying the same argument successively to the subsequences of previous ones on S_2, S_3, S_4, we can choose a subsequence,

call $\{\mathbf{u}_k\}$ again, which converges on each of $S_t, t = 1,2,3,4$. Call its limit $\mathbf{u}^* = (u^*, v^*)$. We claim that $\mathbf{u}^* \in (H^1(T))^2$. Note that $T = \cup_{t=1}^4 S_t$. For simplicity, we assume the interface is a line segment so that $T = T^+ \cup T^-$. The same argument shows that $\mathbf{u}^* \in (H^1(T))^2$ when T consists of four pieces, $T = \cup_{t=1}^4 S_t$. Let us denote $\mathbf{u}_k = (u_k, v_k)$ and $\mathbf{u}^* = (u^*, v^*)$ respectively, and $u_k^s = u_k|_{T^s}, u^s = u^*|_{T^s}, s = +, -$. Let n_1^s be the first component of the unit outer normal vector to the boundary of $T^s, s = +, -$.

By Green's theorem, and the fact $\lim_{k\to\infty} u_k^+ = u^+ = u^-$ on Γ, we get for $\phi \in C_0^\infty(T)$

$$\begin{aligned}\int_{T^+} \frac{\partial u^+}{\partial x}\phi \mathrm{d}x &= \left(\int_{\partial T^+} u^+ n_1^+ \phi \,\mathrm{d}s - \int_{T^+} u^+ \frac{\partial \phi}{\partial x}\mathrm{d}x\right) \\ &= \lim_{k\to\infty}\left(\int_\Gamma u_k^- n_1^+ \phi \,\mathrm{d}s - \int_{T^+} u_k^+ \frac{\partial \phi}{\partial x}\mathrm{d}x\right).\end{aligned}$$

Similarly,

$$\begin{aligned}\int_{T^-} \frac{\partial u^-}{\partial x}\phi \mathrm{d}x &= \left(\int_{\partial T^-} u^- n_1^- \phi \,\mathrm{d}s - \int_{T^-} u^- \frac{\partial \phi}{\partial x}\mathrm{d}x\right) \\ &= \lim_{k\to\infty}\left(\int_\Gamma u_k^- n_1^- \phi \,\mathrm{d}s - \int_{T^-} u_k^- \frac{\partial \phi}{\partial x}\mathrm{d}x\right).\end{aligned}$$

Adding these two equations, we have

$$\int_{T^+} \frac{\partial u^+}{\partial x}\phi \mathrm{d}x + \int_{T^-} \frac{\partial u^-}{\partial x}\phi \mathrm{d}x = -\int_T u^* \frac{\partial \phi}{\partial x}\mathrm{d}x.$$

So if we define the function w by

$$w = \begin{cases} \frac{\partial u_i^+}{\partial x} & \text{on } T^+ \\ \frac{\partial u_i^-}{\partial x} & \text{on } T^- \end{cases}$$

then it satisfies

$$\int_T w\phi \mathrm{d}x = -\int_T u^* \frac{\partial \phi}{\partial x}\mathrm{d}x, \quad \phi \in C_0^\infty(T).$$

This shows $\frac{\partial u^*}{\partial x}$ is well defined in $L^2(T)$. The same argument shows that $\frac{\partial u^*}{\partial y}$ is also well defined in $L^2(T)$. The same argument applied to v^* shows $\mathbf{u}^* = (u^*, v^*) \in (H^1(T))^2$ and hence $\|\mathbf{u}_k - \mathbf{u}^*\|_{1,T} \to 0$. Since

$$\begin{aligned}\|\mathbf{u}_k - \mathbf{u}_l\|_{X(T)}^2 &= \|\mathbf{u}_k - \mathbf{u}_l\|_{1,T}^2 + \|\sqrt{\lambda}\mathrm{div}(\mathbf{u}_k - \mathbf{u}_l)\|_{0,T}^2 + |\!|\!|\mathbf{u}_k - \mathbf{u}_l|\!|\!|_{2,T}^2 \\ &\le \|\mathbf{u}_k - \mathbf{u}^*\|_{1,T}^2 + \|\mathbf{u}^* - \mathbf{u}_l\|_{1,T}^2 \\ &\quad + \|\sqrt{\lambda}\mathrm{div}(\mathbf{u}_k - \mathbf{u}^*)\|_{0,T}^2 + \|\sqrt{\lambda}\mathrm{div}(\mathbf{u}^* - \mathbf{u}_l)\|_{0,T}^2 + (|\!|\!|\mathbf{u}_k|\!|\!|_{2,T} + |\!|\!|\mathbf{u}_l|\!|\!|_{2,T})^2 \to 0\end{aligned}$$

as $k, l \to \infty$, we see that $\{\mathbf{u}_k\}$ is a Cauchy sequence in $X_\Gamma(T)$. By completeness, it converges to a limit in $X_\Gamma(T)$ which is $\mathbf{u}^*$ and hence

$$\|\mathbf{u}^*\|_{X(T)} = \lim_{k\to\infty} \|\mathbf{u}_k\|_{X(T)} = 1. \tag{4.12}$$

Now (4.10), (4.11) gives

$$|\!|\!|\mathbf{u}^*|\!|\!|_{2,T} \le |\!|\!|\mathbf{u}^* - \mathbf{u}_k|\!|\!|_{2,T} + |\!|\!|\mathbf{u}_k|\!|\!|_{2,T} \le C\|\mathbf{u}^* - \mathbf{u}_k\|_{X(T)} + \frac{1}{k} \to 0,$$

this implies $\mathbf{u}^* = 0$. But this is a contradiction to (4.12). □

We define an interpolation operator: for any $\mathbf{u} \in (H^1(T))^2$, we define $I_h\mathbf{u} \in \widehat{\mathbf{N}}_h(T)$ using the average of $\mathbf{u}$ on each edge of T by

$$\int_{e_i} I_h\mathbf{u}\,\mathrm{d}s = \int_{e_i} \mathbf{u}\,\mathrm{d}s, \quad i = 1,2,3$$

and call $I_h\mathbf{u}$ the *interpolant* of $\mathbf{u}$ in $\widehat{\mathbf{N}}_h(T)$. We then define $I_h\mathbf{u}$ for $\mathbf{u} \in (H^1(\Omega))^2$ by $(I_h\mathbf{u})|_T = I_h(\mathbf{u}|_T)$.

Now we are ready to prove the interpolation error estimate.

Lemma 4.4. *For any $\mathbf{u} \in (\widetilde{H}^2_\Gamma(\Omega))^2$, there exists a constant $C > 0$ such that for $m = 0, 1$*

$$\|\mathbf{u} - I_h\mathbf{u}\|_{m,h} + m \cdot \|\sqrt{\lambda}\mathrm{div}(\mathbf{u} - I_h\mathbf{u})\|_{L^2(\Omega)} \le Ch^{2-m}(\|\mathbf{u}\|_{\widetilde{H}^2(\Omega)} + m \cdot \sqrt{\lambda_M}\|\mathrm{div}\mathbf{u}\|_{\widetilde{H}^1(\Omega)}),$$

and

$$\|\mathbf{u} - I_h\mathbf{u}\|_{m,h} \le Ch^{2-m}\|\mathbf{u}\|_{\widetilde{H}^2(\Omega)}.$$

Proof. Let $\check{T}$ be a reference interface element, $\check{\Gamma}$ be the corresponding local reference interface, and $\check{\mathbf{u}}(\check{\mathbf{x}}) := \mathbf{u} \circ \mathbf{F}(\check{\mathbf{x}})$, where $\mathbf{F} : \check{T} \to T$ denote the affine mapping to define the finite element in the real domain. Then for any $\check{\mathbf{u}} \in (\widetilde{H}^2_\Gamma(\check{T}))^2 \subset X_\Gamma(\check{T})$, (let us denote $\check{\mathbf{u}} = (\check{u}_1, \check{u}_2)$ and $I_h\check{\mathbf{u}} = (\check{w}_1, \check{w}_2)$)

$$\begin{aligned}
|||\check{\mathbf{u}} - I_h\check{\mathbf{u}}|||^2_{2,\check{T}} &= |\check{\mathbf{u}} - I_h\check{\mathbf{u}}|^2_{X(\check{T})} + \sum_{s=+,-} |\sqrt{\lambda}\mathrm{div}(\check{\mathbf{u}} - I_h\check{\mathbf{u}})|^2_{1,\check{T}^s} \\
&\quad + \left| \int_{\check{\Gamma}\cap\check{T}} [(\boldsymbol{\sigma}(\check{\mathbf{u}}) - \boldsymbol{\sigma}(I_h\check{\mathbf{u}})) \cdot \mathbf{n}_\Gamma]\,\mathrm{d}s \right|^2 + \sum_{i=1}^{3} |(\overline{\check{u}_1 - \check{w}_1})|_{e_i}|^2 + \sum_{i=1}^{3} |(\overline{\check{u}_2 - \check{w}_2})|_{e_i}|^2 \\
&= |\check{\mathbf{u}} - I_h\check{\mathbf{u}}|^2_{X(\check{T})} + \sum_{s=+,-} |\sqrt{\lambda}\mathrm{div}(\check{\mathbf{u}} - I_h\check{\mathbf{u}})|^2_{1,\check{T}^s} = |\check{\mathbf{u}}|^2_{X(\check{T})} + \sum_{s=+,-} |\sqrt{\lambda}\mathrm{div}\,\check{\mathbf{u}}|^2_{1,\check{T}^s},
\end{aligned}$$

where we used the properties of the interpolation operator I_h, Lemma 4.2, and the fact that H^2-seminorm of the piecewise linear function $I_h\check{\mathbf{u}}$ vanishes.

Let $m = 0$ or 1. By Lemma 4.3 and scaling argument,

$$\begin{aligned}
\|\mathbf{u} - I_h\mathbf{u}\|_{b,m,T} &\le Ch^{1-m}\|\check{\mathbf{u}} - I_h\check{\mathbf{u}}\|_{b,m,\check{T}} \\
&\le Ch^{1-m}\|\check{\mathbf{u}} - I_h\check{\mathbf{u}}\|_{X(\check{T})} \\
&\le Ch^{1-m}|||\check{\mathbf{u}} - I_h\check{\mathbf{u}}|||_{2,\check{T}} \\
&= Ch^{1-m}(|\check{\mathbf{u}}|_{X(\check{T})} + m \cdot \sum_{s=+,-} |\sqrt{\lambda}\mathrm{div}\,\check{\mathbf{u}}|_{1,\check{T}^s}) \\
&\le Ch^{2-m}(|\mathbf{u}|_{X(T)} + m \cdot \sum_{s=+,-} |\sqrt{\lambda}\mathrm{div}\,\mathbf{u}|_{1,T^s}) \\
&\le Ch^{2-m}(\|\mathbf{u}\|_{\widetilde{H}^2(T)} + m \cdot \sum_{s=+,-} |\sqrt{\lambda}\mathrm{div}\,\mathbf{u}|_{1,T^s}).
\end{aligned}$$

For the second assertion one can proceed exactly the same way without the terms involving div$\mathbf{u}$ in the definition of norms $\|\cdot\|_{b,m,T}, \|\cdot\|_{X(T)}$ and $|||\cdot|||_{2,T}$ to obtain the desired estimate. □

Lemma 4.5. *Let $\mathbf{u} \in (\widetilde{H}^2_\Gamma(\Omega))^2$. We have*

$$\|\mathbf{u} - I_h\mathbf{u}\|_{a_h} \le Ch\left(\|\mathbf{u}\|_{\widetilde{H}^2(\Omega)} + \sqrt{\lambda_M}\|\mathrm{div}\mathbf{u}\|_{\widetilde{H}^1(\Omega)}\right), \tag{4.13}$$

for some constant $C > 0$.

Proof. Recall that

$$\|\mathbf{u}-I_h\mathbf{u}\|_{a_h}^2 = \sum_{T\in\mathcal{T}_h}\int_T \left(2\mu\epsilon(\mathbf{u}-I_h\mathbf{u}):\epsilon(\mathbf{u}-I_h\mathbf{u})+\lambda|\mathrm{div}(\mathbf{u}-I_h\mathbf{u})|^2\right)\mathrm{d}x + \sum_{e\in\mathcal{E}}\int_e \frac{\tau}{h}[\mathbf{u}-I_h\mathbf{u}]^2\mathrm{d}s.$$

Clearly, the terms in the first summation are bounded by the $\|\mathbf{u}-I_h\mathbf{u}\|_{b,1,T}$ for each element. Hence these are bounded by right hand side of (4.13) by Lemma 4.4. For the second term, we have

$$\frac{1}{h}\|[\mathbf{u}-I_h\mathbf{u}]\|_{0,e}^2 \le \frac{1}{h}\|\mathbf{u}-I_h\mathbf{u}\|_{0,e}^2 \tag{4.14}$$

$$\le C\left(\frac{1}{h^2}\|\mathbf{u}-I_h\mathbf{u}\|_{0,T}^2+|\mathbf{u}-I_h\mathbf{u}|_{1,T}^2\right) \tag{4.15}$$

$$\le Ch^2\|\mathbf{u}\|_{\tilde{H}^2(T)}^2, \tag{4.16}$$

by trace inequality and Lemma 4.4. This completes the proof. □

4.2. Consistency error estimate

For consistency error estimate, we need the following lemma.

Lemma 4.6 (Korn's inequality [10, 16]). *There exists constant $C>0$ such that*

$$|\mathbf{v}_h|_{1,h}^2 \le C\sum_{T\in\mathcal{T}_h}(\|\boldsymbol{\epsilon}(\mathbf{v}_h)\|_{0,T}^2+\|Q(\mathbf{v}_h)\|_{0,T}^2)+\sum_{e\in\mathcal{E}}\int_e\frac{\tau}{h}[\mathbf{v}_h]^2\mathrm{d}s, \forall\mathbf{v}_h\in\widehat{\mathbf{N}}(T), \tag{4.17}$$

where $Q(\mathbf{v}_h):=\mathbf{v}_h-\frac{1}{|T|}\int_T\mathbf{v}_h\,\mathrm{d}x$.

Corollary 4.7. *The form $a_h(\cdot,\cdot)$ is a norm equivalent to $\|\cdot\|_{1,h}$.*

Proof. There exists a constant $C(T)>0$ such that the following holds.

$$\|Q(\mathbf{v}_h)\|_{0,T}^2 \le C(T)h|\mathbf{v}_h|_{1,T}^2.$$

Hence by Lemma 4.6, we have

$$|\mathbf{v}_h|_{1,h}^2 \le C\sum_{T\in\mathcal{T}_h}\left(\|\boldsymbol{\epsilon}(\mathbf{v}_h)\|_{0,T}^2+\int_T\lambda|\mathrm{div}\mathbf{v}_h|^2\mathrm{d}x\right)+\sum_{e\in\mathcal{E}}\int_e\frac{\tau}{h}[\mathbf{v}_h]^2\mathrm{d}s, \quad \text{for all } \mathbf{v}_h\in\widehat{\mathbf{N}}(T)$$

holds for sufficiently small h. Hence by Poincaré inequality for CR finite element spaces [23], we get the result. □

Lemma 4.8. *Let $\mathbf{u}\in\tilde{H}^2(\Omega)$ be the solution of (2.1). We assume $\sigma(\mathbf{u})\cdot\mathbf{n}\in(H^1(T))^2$ for each T. Then following inequality holds:*

$$|a_h(\mathbf{u},\mathbf{v}_h)-a_h(\mathbf{u}_h,\mathbf{v}_h)| \le ChR(\mathbf{u})\|\mathbf{v}_h\|_{a_h},$$

where

$$R(\mathbf{u}) = \|\mathbf{u}\|_{\tilde{H}^2(\Omega)}+\lambda_M\|\mathrm{div}\mathbf{u}\|_{\tilde{H}^1(\Omega)}.$$

Proof. First we note that the consistency error term is

$$\begin{aligned}|a_h(\mathbf{u},\mathbf{v}_h)-a_h(\mathbf{u}_h,\mathbf{v}_h)| &= |a_h(\mathbf{u},\mathbf{v}_h)-\mathbf{f}(\mathbf{v}_h)|\\ &= \Bigg|\sum_{T\in\mathcal{T}_h}\int_T 2\mu\epsilon(\mathbf{u}):\epsilon(\mathbf{v}_h)+\sum_{T\in\mathcal{T}_h}\int_T\lambda\mathrm{div}\mathbf{u}\,\mathrm{div}\mathbf{v}_h+\sum_{e\in\mathcal{E}}\int_e\frac{2\mu}{h}[\mathbf{u}][\mathbf{v}_h]\,\mathrm{d}s\\ &\quad -\sum_{T\in\mathcal{T}_h}(\mathrm{div}\boldsymbol{\sigma}(\mathbf{u}),\mathbf{v}_h)_T\Bigg|.\end{aligned}$$

Using integration by parts we see the first two summations cancel and that

$$|a_h(\mathbf{u},\mathbf{v}_h)-a_h(\mathbf{u}_h,\mathbf{v}_h)| = \left|\sum_{T\in\mathcal{T}_h}\sum_{e\subset\partial T}\int_e \boldsymbol{\sigma}(\mathbf{u})\mathbf{n}\cdot[\mathbf{v}_h]\mathrm{d}s\right|,$$

since $[\mathbf{u}]=0$. Using the technique in [17] (Lem. 3, p. 41), we see that

$$\begin{aligned}\left|\sum_{T\in\mathcal{T}_h}\sum_{e\subset\partial T}\int_e (\boldsymbol{\sigma}(\mathbf{u})\mathbf{n}-\overline{\boldsymbol{\sigma}(\mathbf{u})\mathbf{n}})\cdot[\mathbf{v}_h]\mathrm{d}s\right| &\le Ch\sum_{T\in\mathcal{T}_h}\|\boldsymbol{\sigma}(\mathbf{u})\mathbf{n}\|_{1,T}|\mathbf{v}_h|_{1,T}\\ &\le Ch(\|\mathbf{u}\|_{\tilde{H}^2(\Omega)}+\lambda_M\|\mathrm{div}\mathbf{u}\|_{\tilde{H}^1(\Omega)})\|\mathbf{v}_h\|_{a_h}\end{aligned}$$

by Corollary 4.7. □

Now we are ready to prove the H^1-error estimate.

Theorem 4.9. *Let* $\mathbf{u}$ (resp. $\mathbf{u}_h$) *be the solution of* (2.1)(resp. (3.5)). *Under the assumption that* $\sigma(\mathbf{u})\cdot\mathbf{n}\in(H^1(\Omega))^2$, *we have*

$$\|\mathbf{u}-\mathbf{u}_h\|_{a_h} \le Ch\left(\|\mathbf{u}\|_{\tilde{H}^2(\Omega)}+\lambda_M\|\mathrm{div}\mathbf{u}\|_{\tilde{H}^1(\Omega)}\right).$$

Proof. By triangular inequality, we have

$$\|\mathbf{u}-\mathbf{u}_h\|_{a_h} \le \|\mathbf{u}_h-I_h\mathbf{u}\|_{a_h}+\|\mathbf{u}-I_h\mathbf{u}\|_{a_h}.$$

We have

$$\begin{aligned}\|\mathbf{u}_h-I_h\mathbf{u}\|_{a_h}^2 &= a_h(\mathbf{u}_h-I_h\mathbf{u},\mathbf{u}_h-I_h\mathbf{u})\\ &= a_h(\mathbf{u}-I_h\mathbf{u},\mathbf{u}_h-I_h\mathbf{u})+a_h(\mathbf{u}_h-\mathbf{u},\mathbf{u}_h-I_h\mathbf{u})\\ &\le \|\mathbf{u}_h-I_h\mathbf{u}\|_{a_h}\|\mathbf{u}-I_h\mathbf{u}\|_{a_h}+ChR(\mathbf{u})\|\mathbf{u}_h-I_h\mathbf{u}\|_{a_h},\end{aligned}$$

by Lemma 4.8. So we have

$$\|\mathbf{u}_h-I_h\mathbf{u}\|_{a_h} \le \|\mathbf{u}-I_h\mathbf{u}\|_{a_h}+ChR(\mathbf{u}).$$

Finally, by Lemma 4.5 we have

$$\|\mathbf{u}-\mathbf{u}_h\|_{a_h} \le 2\|\mathbf{u}-I_h\mathbf{u}\|_{a_h}+ChR(\mathbf{u}) \le C_1hR(\mathbf{u}).$$ □

Remark 4.10. If the H^2-stability of the continuous problem holds, *i.e.*, $\|\mathbf{u}\|_{\tilde{H}^2(\Omega)}+\lambda_M\|\mathrm{div}\mathbf{u}\|_{\tilde{H}^1(\Omega)} \le C\|f\|_0$, then the result of Theorem 4.9 improves to

$$\|\mathbf{u}-\mathbf{u}_h\|_{a_h} \le Ch\|f\|_0.$$

This would mean that our estimate holds as $\lambda\to\infty$ also. Furthermore, by standard duality argument, we can obtain L^2- error estimate of the form:

$$\|\mathbf{u}-\mathbf{u}_h\|_0 \le Ch^2\|f\|_0.$$

TABLE 1. $\mu^- = 1,\ \mu^+ = 100, \lambda = 5\mu$.

$1/h$	$\|\mathbf{u} - \mathbf{u}_h\|_0$	Order	$\|\mathbf{u} - \mathbf{u}_h\|_{1,h}$	Order	$\|\mathrm{div}\mathbf{u} - \mathrm{div}\mathbf{u}_h\|_0$	Order
8	1.887e-3		4.098e-2		4.694e-2	
16	5.354e-4	1.817	1.957e-2	1.066	2.311e-2	1.022
32	1.186e-4	2.175	9.547e-3	1.036	1.089e-2	1.085
64	2.864e-5	2.050	4.850e-3	0.977	5.382e-3	1.017
128	6.793e-6	2.076	2.430e-3	0.997	2.637e-3	1.029
256	1.673e-6	2.021	1.217e-3	0.998	1.310e-3	1.009

TABLE 2. $\mu^- = 1,\ \mu^+ = 10, \lambda = 5\mu$.

$1/h$	$\|\mathbf{u} - \mathbf{u}_h\|_0$	Order	$\|\mathbf{u} - \mathbf{u}_h\|_{1,h}$	Order	$\|\mathrm{div}\mathbf{u} - \mathrm{div}\mathbf{u}_h\|_0$	Order
8	2.910e-3		7.972e-2		8.598e-2	
16	7.450e-4	1.966	3.822e-2	1.061	4.155e-2	1.049
32	1.841e-4	2.017	1.942e-2	0.977	2.091e-2	0.991
64	4.606e-5	1.999	9.787e-3	0.989	1.049e-2	0.996
128	1.143e-5	2.010	4.920e-3	0.992	5.255e-3	0.997
256	2.851e-6	2.004	2.466e-3	0.997	2.630e-3	0.999

5. Numerical results

In this section we present numerical examples. The domain is $\Omega = (-1,1)\times(-1,1)$. The interface is the zero set of $L(x,y) = x^2 + y^2 - r_0^2$. Let $\Omega^+ = \Omega \cap \{(x,y)|L(x,y) > 0\}$, $\Omega^- = \Omega \cap \{(x,y)|L(x,y) < 0\}$. The exact solution is chosen as

$$\mathbf{u} = \left(\frac{1}{\mu}(x^2 + y^2 - r_0^2)x, \frac{1}{\mu}(x^2 + y^2 - r_0^2)y\right)$$

with various values of μ and λ. For numerical simulation we partition the domain into uniform right triangles having size $h = 2^{-k}, k = 3, 4, \ldots$

Example 5.1. In this example, we test two sets of parameters and radii of the interface.

1. We choose $\mu^- = 1,\ \mu^+ = 100, \lambda = 5\mu$ and $r_0 = 0.36$.
2. We choose $\mu^- = 1,\ \mu^+ = 10, \lambda = 5\mu$ and $r_0 = 0.48$.

Tables 1 and 2 show the convergence behavior of our numerical schemes for both examples. In both cases, we see the optimal order of convergence in L^2, H^1 and divergence norms. x-components of the solution are plotted in Figures 4 and 5.

We provide a detailed illustration of the solution in a neighborhood of the interface when small cut elements exist with $\mu^- = 1,\ \mu^+ = 100, \lambda = 5\mu$. Figures 6a and 6c show some elements with small cuts, while Figures 6b and 6d show the solution graphs near the interface. We see no roughness at all. We observe similar behavior for all other examples. We see the numerical solutions also behave well when the Lamé constants have large contrasts, $\mu^+/\mu^- = 100$.

Example 5.2 (Nearly incompressible case)**.**

(1) We let $\mu^- = 1,\ \mu^+ = 10, \lambda = 100\mu, \nu = 0.495$ and $r_0 = 0.7$.
(1) We let $\mu^- = 1,\ \mu^+ = 10, \lambda = 1000\mu, \nu = 0.4995$ and $r_0 = 0.6$.

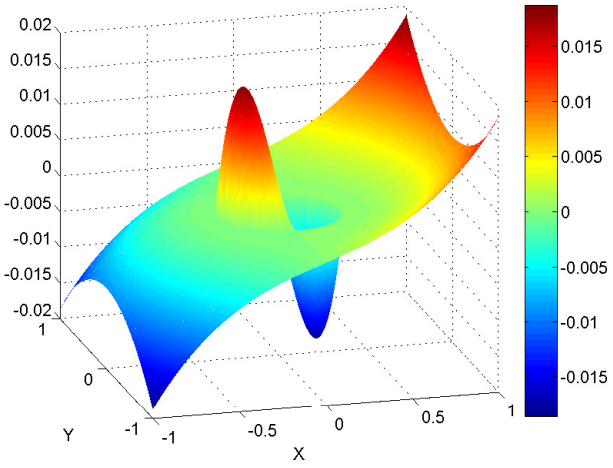

FIGURE 4. x-component, $\mu^- = 1,\ \mu^+ = 100, \lambda = 5\mu$.

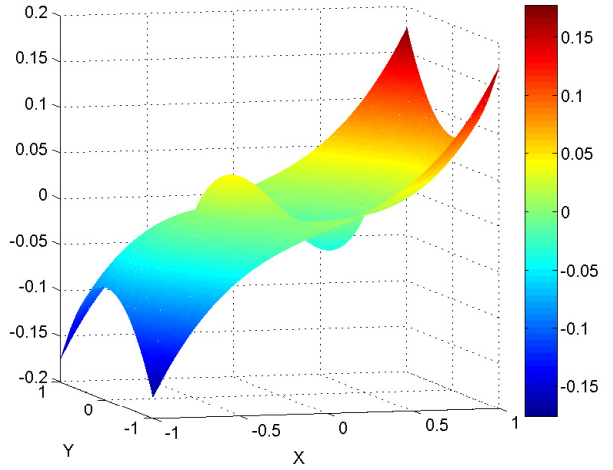

FIGURE 5. x-component, $\mu^- = 1,\ \mu^+ = 10, \lambda = 5\mu$.

Tables 3 and 4 show the convergence behavior. In both cases, we see the optimal order of convergence in L^2, H^1 and divergence norms. No locking phenomena occurs in both cases. Again x-components of the solution are plotted in Figures 7 and 8. In this example, the ratio $\lambda : \mu$ is $100 : 1$ and $1000 : 1$. These correspond to nearly incompressible case.

Example 5.3 (Ellipse interface case)**.** Next we consider examples with elliptic shaped interface. The domain is the same as above, and the interface is represented by $L(x, y) = \frac{x^2}{4} + y^2 - r_0^2 = 0$. The exact solution is chosen as

$$\mathbf{u} = \left(\frac{1}{\mu}\left(\frac{x^2}{4} + y^2 - r_0^2\right)x, \frac{1}{\mu}\left(\frac{x^2}{4} + y^2 - r_0^2\right)y\right)$$

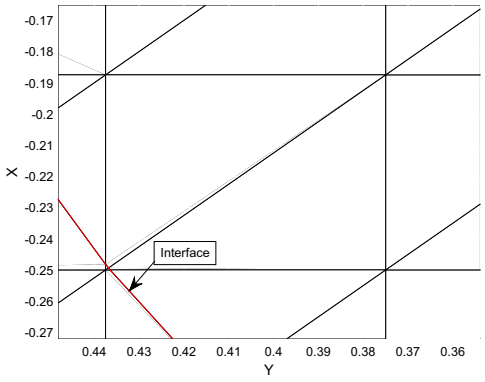

(a) neighborhood of the interface with small cuts

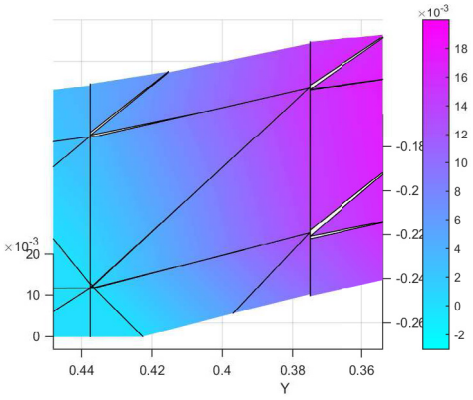

(b) The x-component of solution of (a)

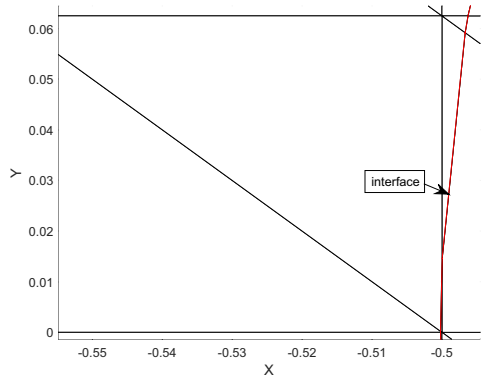

(c) neighborhood of the interface when thin cuts

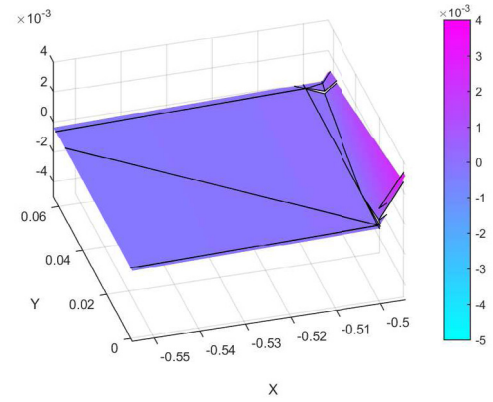

(d) The x-component of solution of (c)

FIGURE 6. Elements with small/thin cuts and solutions near interface.

TABLE 3. $\mu^- = 1,\ \mu^+ = 10, \lambda = 100\mu$.

$1/h$	$\|\mathbf{u}-\mathbf{u}_h\|_0$	Order	$\|\mathbf{u}-\mathbf{u}_h\|_{1,h}$	Order	$\|\mathrm{div}\mathbf{u}-\mathrm{div}\mathbf{u}_h\|_0$	Order
8	7.733e-3		1.456e-1		2.132e-1	
16	2.487e-3	1.644	7.541e-2	0.949	1.136e-1	0.909
32	7.434e-4	1.742	3.729e-2	1.016	5.527e-2	1.039
64	2.124e-4	1.807	1.876e-2	0.991	2.730e-2	1.018
128	5.508e-5	1.948	9.417e-3	0.994	1.347e-2	1.019
256	1.428e-5	1.948	4.719e-3	0.997	6.686e-3	1.011

with various values of μ and λ.

(1) We let $\mu^- = 1,\ \mu^+ = 10, \lambda = 5\mu, r_0 = 0.4$.
(2) We let $\mu^- = 1,\ \mu^+ = 100, \lambda = 5\mu, r_0 = 0.3$.

Tables 5 and 6 show the convergence behavior. We observe similar optimal convergence rates for all norms. Figures 9 and 10 show the x-components of the solution.

TABLE 4. $\mu^- = 1,\ \mu^+ = 10, \lambda = 1000\mu$.

$1/h$	$\|\mathbf{u} - \mathbf{u}_h\|_0$	Order	$\|\mathbf{u} - \mathbf{u}_h\|_{1,h}$	Order	$\|\mathrm{div}\mathbf{u} - \mathrm{div}\mathbf{u}_h\|_0$	Order
8	7.655e-2		1.125e-1		1.628e-0	
16	2.372e-2	1.690	5.570e-2	1.014	9.065e-1	0.846
32	6.806e-2	1.801	2.829e-2	0.978	4.518e-1	1.004
64	1.847e-3	1.882	1.417e-2	0.997	2.247e-1	1.008
128	4.811e-4	1.941	7.110e-3	0.995	1.111e-1	1.016
256	1.230e-4	1.968	3.563e-3	0.997	5.534e-2	1.006

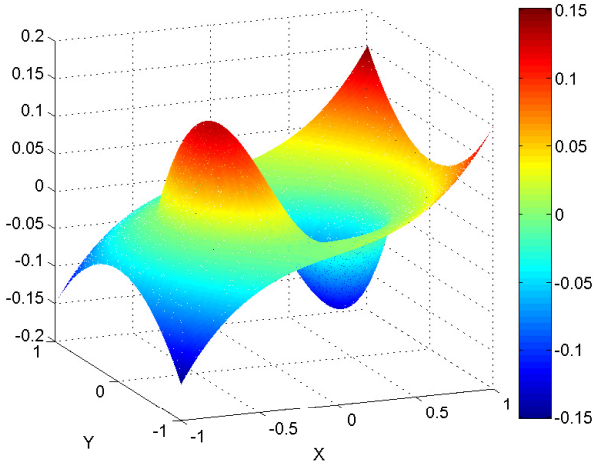

FIGURE 7. x-component, $\mu^- = 1,\ \mu^+ = 10, \lambda = 100\mu$.

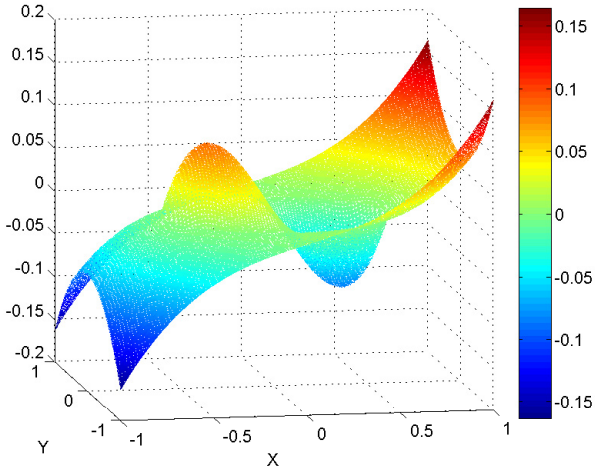

FIGURE 8. x-component, $\mu^- = 1,\ \mu^+ = 10, \lambda = 1000\mu$.

TABLE 5. $\mu^- = 1,\ \mu^+ = 10, \lambda = 5\mu$, elliptical interface.

$1/h$	$\|\mathbf{u}-\mathbf{u}_h\|_0$	Order	$\|\mathbf{u}-\mathbf{u}_h\|_{1,h}$	Order	$\|\mathrm{div}\mathbf{u}-\mathrm{div}\mathbf{u}_h\|_0$	Order
8	2.477e-3		5.920e-2		6.744e-2	
16	6.689e-4	1.888	2.909e-2	1.025	3.340e-2	1.014
32	1.704e-4	1.973	1.480e-2	0.975	1.694e-2	0.979
64	4.200e-5	2.020	7.485e-3	0.983	8.531e-3	0.990
128	1.029e-5	2.029	3.765e-3	0.992	4.281e-3	0.995
256	2.579e-6	1.996	1.886e-3	0.997	2.144e-3	0.998

TABLE 6. $\mu^- = 1,\ \mu^+ = 100, \lambda = 5\mu$, elliptical interface.

$1/h$	$\|\mathbf{u}-\mathbf{u}_h\|_0$	Order	$\|\mathbf{u}-\mathbf{u}_h\|_{1,h}$	Order	$\|\mathrm{div}\mathbf{u}-\mathrm{div}\mathbf{u}_h\|_0$	Order
8	2.018e-3		3.164e-2		3.788e-2	
16	6.644e-4	1.647	1.424e-2	1.151	2.066e-2	0.875
32	1.376e-4	2.227	7.314e-3	0.962	9.592e-3	1.107
64	2.736e-5	2.330	3.735e-3	0.969	4.458e-3	1.105
128	6.896e-6	1.988	1.880e-3	0.991	2.229e-3	1.000
256	1.726e-6	1.998	9.434e-4	0.994	1.107e-3	1.010

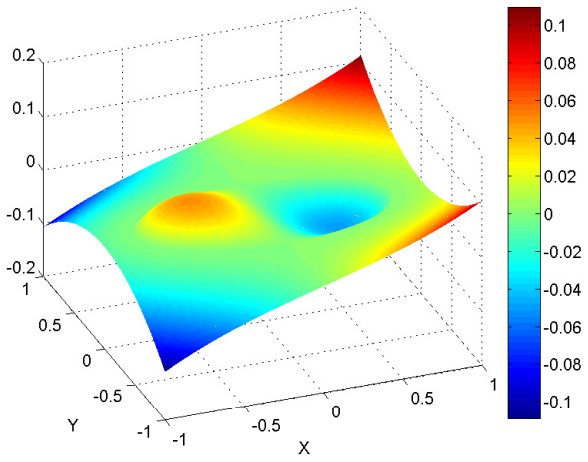

FIGURE 9. x-component, $\mu^- = 1,\ \mu^+ = 10, \lambda = 5\mu$ elliptical interface.

Example 5.4 (Unknown solution)**.** This last example computes a problem with unknown solution. We choose $\mu^- = 1,\ \mu^+ = 100, \nu^- = 0.28, \nu^+ = 0.4, r_0 = 0.3$ and $\mathbf{F} = \left(-\frac{11}{4} - \frac{\lambda}{\mu}x, -\frac{29}{4} - \frac{\lambda}{\mu}y\right)$ with the same elliptical interface as in the previous example.

Figure 11 shows the x-component of the computed solution.

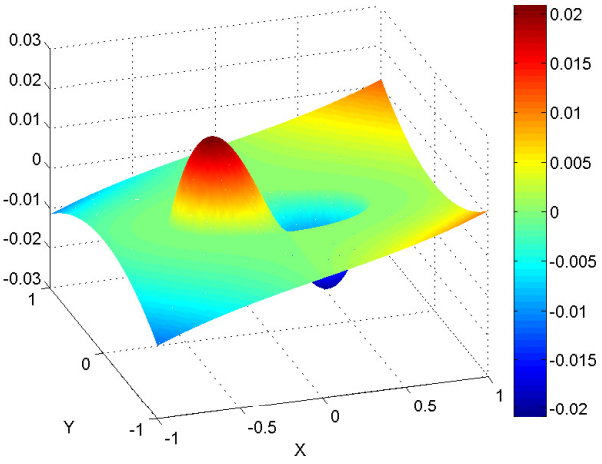

FIGURE 10. x-component, $\mu^- = 1,\ \mu^+ = 100, \lambda = 5\mu$ elliptical interface.

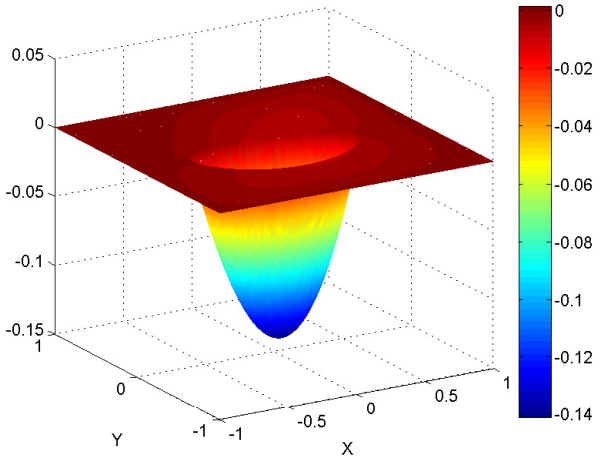

FIGURE 11. x-component, $\mu^- = 1,\ \mu^+ = 100, \nu^- = 0.28, \nu^+ = 0.4, r_0 = 0.3$ unknown solution.

6. Conclusion

In the present work, we have developed a new finite element method for solving planar elasticity problems with an interface along which distinct materials are bonded. The methods are based on the IFEM using CR element modified to satisfy Laplace–Young condition along the interface. Our methods yield smaller matrix size than XFEM since we do not use any extra dofs other than the edge based functions. The jump terms along the edges are added to ensure the stability of the scheme.

We have proved an interpolation error in H^1 and $H(\mathrm{div})$ norm (with $\sqrt{\lambda}$ factor). For the error estimate of $\mathbf{u} - \mathbf{u}_h$, we have obtained an optimal $O(h)$ error in H^1 and $H(\mathrm{div})$ norm under the regularity that $\boldsymbol{\sigma}(\mathbf{u}) \in (H^1(\Omega))^2$. The numerical tests show the optimal $O(h)$ error in H^1 norm, and $O(h^2)$ in L^2 norm.

As future works, we will consider nonhomogeneous jump conditions and three dimensional problems.

Appendix A

We sketch the proof of Proposition 3.2. The degrees of freedom and point continuity of (3.4) give rise to the ten equations for the coefficients of $\hat{\phi}_1$ and $\hat{\phi}_2$, in the form

$$\begin{pmatrix} A & \mathbf{0} \\ \mathbf{0} & A \end{pmatrix} \begin{pmatrix} \mathbf{c}_1 \\ \mathbf{c}_2 \end{pmatrix} = \begin{pmatrix} \mathbf{g}_1 \\ \mathbf{g}_2 \end{pmatrix} \tag{A.1}$$

where

$$A = \begin{pmatrix} 1 & \frac{1}{2} & \frac{1}{2} & 0 & 0 & 0 \\ 1-y & 0 & \frac{1}{2}(1-y^2) & y & 0 & \frac{1}{2}y^2 \\ 1-x & \frac{1}{2}(1-x^2) & 0 & x & \frac{1}{2}x^2 & 0 \\ -1 & -x & 0 & 1 & x & 0 \\ -1 & 0 & -y & 1 & 0 & y \end{pmatrix} \tag{A.2}$$

and $\mathbf{c}_i = (a_i^+, b_i^+, c_i^+, a_i^-, b_i^-, c_i^-)$, $i = 1, 2$ are the vector of the unknowns. The jump conditions along the interface (last equations of (3.4)) give rise to the following equations.

$$\begin{aligned} \mu^+ \begin{pmatrix} b_1^+ & c_1^+ \\ b_2^+ & c_2^+ \end{pmatrix} \cdot \mathbf{n} - \mu^- \begin{pmatrix} b_1^- & c_1^- \\ b_2^- & c_2^- \end{pmatrix} \cdot \mathbf{n} + \mu^+ \begin{pmatrix} b_1^+ & b_2^+ \\ c_1^+ & c_2^+ \end{pmatrix} \cdot \mathbf{n} - \mu^- \begin{pmatrix} b_1^- & b_2^- \\ c_1^- & c_2^- \end{pmatrix} \cdot \mathbf{n} \\ + \lambda^+(b_1^+ + c_2^+)\mathbf{n} - \lambda^-(b_1^- + c_2^-)\mathbf{n} = 0. \end{aligned} \tag{A.3}$$

Combining (A.1) and (A.3), we get the following system of twelve equations in twelve unknowns.

$$M = \begin{pmatrix} A & \mathbf{0} \\ \mathbf{d}_1^T & \mathbf{d}_2^T \\ \mathbf{0} & A \\ \mathbf{e}_1^T & \mathbf{e}_2^T \end{pmatrix} \begin{pmatrix} \mathbf{c}_1 \\ \mathbf{c}_2 \end{pmatrix} = \begin{pmatrix} \mathbf{g}_1 \\ 0 \\ \mathbf{g}_2 \\ 0 \end{pmatrix}. \tag{A.4}$$

Here

$$\begin{aligned} \mathbf{d}_1^T &= \big(0, (2\mu^+ + \lambda^+)n_1, \mu^+ n_2, 0, -(2\mu^- + \lambda^-)n_1, -\mu^- n_2\big) := (d_{1i})_{i=1}^6, \\ \mathbf{d}_2^T &= \big(0, \mu^+ n_2, \lambda^+ n_1, 0, -\mu^- n_2, -\lambda^- n_1\big) := (d_{2i})_{i=1}^6 \\ \mathbf{e}_1^T &= \big(0, \lambda^+ n_2, \mu^+ n_1, 0, -\lambda^- n_2, -\mu^- n_1\big) := (e_{1i})_{i=1}^6 \\ \mathbf{e}_2^T &= \big(0, \mu^+ n_1, (2\mu^+ + \lambda^+)n_2, 0, -\mu^- n_1, -(2\mu^- + \lambda^-)n_2\big) := (e_{2i})_{i=1}^6. \end{aligned}$$

Now we will compute the determinant of M. Adding columns 6,5,4 to 3,2,1 and columns 12,11,10 to 9,8,7 (resp.), and by row eliminations, we obtain following.

$$M' := \left(\begin{array}{ccc|ccc} U & & 0 & \mathbf{O} & & 0 \\ & & & & & \\ 0 & & \bar{d}_{66} & \bar{\mathbf{d}_2}^T & & 0 \\ \hline \mathbf{O} & & 0 & U & & 0 \\ & & & & & \\ 0 & & \bar{e}_{16} & 0 & & \bar{e}_{66} \end{array}\right), \text{ where } U = \begin{pmatrix} 1 & \frac{1}{2} & \frac{1}{2} & 0 & 0 \\ 0 & -\frac{1}{2} & 0 & y & 0 \\ 0 & 0 & -\frac{1}{2} & x & \frac{1}{2}x^2 \\ 0 & 0 & 0 & 1 & x \\ 0 & 0 & 0 & 0 & -x \end{pmatrix}. \tag{A.5}$$

Here $\bar{d}_{66}, \bar{e}_{16}$ and $\bar{e}_{66}$ are given by

$$\begin{aligned} x\bar{d}_{66} &= -n_1 y\{(2\mu^+ + \lambda^+)xy + (2\mu^- + \lambda^-)(1-xy)\} - xn_2\{\mu^+ xy + \mu^-(1-xy)\}, \\ x\bar{e}_{16} &= -n_2 y\{\lambda^+ xy + \lambda^-(1-xy)\} - n_1 x\{\mu^+ xy + \mu^-(1-xy)\}, \\ x\bar{e}_{66} &= -yn_1\{\mu^+ xy + \mu^-(1-xy)\} - xn_2\{(2\mu^- + \lambda^-)(1-xy) + (2\mu^+ + \lambda^+)xy\}. \end{aligned}$$

Lemma A.1. *The determinant of matrix M' is given as follows.*

$$\det(M') = \frac{1}{16}\left\{x\bar{d}_{66}x\bar{e}_{66} - 4x\bar{e}_{16}\cdot cofac\right\}. \tag{A.6}$$

Here, with the notation $[\lambda] = \lambda^+ - \lambda^-, [\lambda] = \lambda^+ - \lambda^-$, cofac is given by

$$cofac = -\frac{1}{4}\left([\mu]n_2xy^2 + [\lambda]n_1x^2y + x\lambda^- n_1 + y\mu^- n_2\right).$$

Proof. This can be obtained by expanding the determinant with resp. to fifth column of M'. □

Proposition A.2. *The determinant of matrix M' is always negative.*

Proof. Substituting $(n_1, n_2) = \frac{(y,x)}{\sqrt{x^2+y^2}}$ into (A.6) we see

$$\begin{aligned}
-16\sqrt{x^2+y^2}\det(M') &= \left\{y^2\{(2\mu^+ + \lambda^+)xy + (2\mu^- + \lambda^-)(1-xy)\} + x^2\{\mu^+xy + \mu^-(1-xy)\}\right\} \\
&\quad \times \left\{y^2\{\mu^+xy + \mu^-(1-xy)\} + x^2\{(2\mu^- + \lambda^-)(1-xy) + (2\mu^+ + \lambda^+)xy\}\right\} \\
&\quad + \bar{e}_{16}x(([\mu] + [\lambda])x^2y^2 + (\lambda^- + \mu^-)xy) \\
&= \left\{y^2([2\mu + \lambda]xy + (2\mu^- + \lambda^-)) + x^2([\mu]xy + \mu^-)\right\} \\
&\quad \times \left\{y^2([\mu]xy + \mu^-) + x^2([2\mu + \lambda]xy + (2\mu^- + \lambda^-))\right\} \\
&\quad - (xy)^2(([\mu] + [\lambda])xy + (\lambda^- + \mu^-))^2 \\
&= y^4A(2A+B) + x^4A(2A+B) + x^2y^2\{(2A+B)^2 + A^2\} - (xy)^2(A+B)^2 > 0
\end{aligned}$$

where $A = [\mu]xy + \mu^-, B = [\lambda]xy + \lambda^-$. Hence the determinant is always negative. □

References

[1] D.N. Arnold, An interior penalty finite element method with discontinuous elements. *SIAM J. Numer. Anal.* **19** (1982) 742–760.

[2] D.N. Arnold and R. Winther, Mixed finite elements for elasticity. *Numer. Math.* **92** (2002) 401–419.

[3] D.N. Arnold, F. Brezzi, B. Cockburn and D. Marini, Discontinuous Galerkin methods for elliptic problems, in *Discontinuous Galerkin Methods. Theory.* In vol. 11 of *Computation and Applications*, edited by B. Cockburn, G.E. Karniadakis and C.-W. Shu. *Lecture Notes Comput. Sci. Engrg.* Springer-Verlag, New York (2000) 89–101.

[4] I. Babuška and M. Suri, Locking effect in the finite element approximation of elasticity problem. *Numer. Math.* **62** (1992) 439–463.

[5] I. Babuška and M. Suri, On locking and robustness in the finie element method. *SIAM J. Numer. Anal.* **29** (1992) 1261–1293.

[6] R. Becker, E. Burman and P. Hansbo, A Nitsche extended finite element method for incompressible elasticity with discontinuous modulus of elasticity. *Comput. Methods Appl. Mech. Engrg.* **198** (2009) 3352–3360.

[7] T. Belytschko and T. Black, Elastic crack growth in finite elements with minimal remeshing. *Int. J. Numer. Meth. Engrg.* **45** (1999) 601–620.

[8] T. Belytschko, C. Parimi, N. Moës, N. Sukumar and S. Usui, Structured extended finite element methods for solids defined by implicit surfaces. *Int. J. Numer. Meth. Engrg.* **56** (2003) 609–635.

[9] D. Braess, *Finite elements: Theory, fast solvers, and applications in solid mechanics*, 2nd edition. Cambridge University Press, Cambridge (2001).

[10] S.C. Brenner, Korn's inequalities for piecewise H^1 vector fields. *Math. Comp.* **72** (2003) 1067–1087.

[11] S.C. Brenner and L.Y. Sung, Linear finite element methods for planar linear elasticity. *Math. Comp.* **59** (1992) 321–338.

[12] F. Brezzi and M. Fortin, *Mixed and hybrid finite element methods*. Springer-Verlag, New-York (1991).

[13] K.S. Chang and D.Y. Kwak, Discontinuous Bubble scheme for elliptic problems with jumps in the solution. *Comput. Method Appl. Mech. Engrg.* **200** (2011) 494–508.

[14] S.H. Chou, D.Y. Kwak and K.T. Wee, Optimal convergence analysis of an immersed interface finite element method. *Adv. Comput. Math.* **33** (2010) 149–168.

[15] P.G. Ciarlet, *The finite element method for elliptic problems*. North Holland (1978).

[16] P.G. Ciarlet, *Mathematical elasticity*. Vol I. North Holland (1988).

[17] M. Crouzeix and P.A. Raviart, Conforming and nonconforming finite element methods for solving the stationary Stokes equations. *RAIRO Anal. Numér.* **7** (1973) 33–75.

[18] R.S. Falk, Nonconforming Finite Element Methods for the Equations of Linear Elasticity. *Math. Comput.* **57** (1991) 529–550.

[19] A. Hansbo and P. Hansbo, An unfitted finite element method, based on Nitsche's method, for elliptic interface problems. *Comput. Methods Appl. Mech. Engrg.* **191** (2002) 5537–5552.

[20] A. Hansbo and P. Hansbo, A finite element method for the simulation of strong and weak discontinuities in solid mechanics. *Comput. Methods Appl. Mech. Engrg.* **193** (2004) 3523–3540.

[21] P. Hansbo and M.G. Larson, Discontinuous Galerkin and the Crouzeix–Raviart element: Applications to elasticity. *ESAIM: M2AN* **37** (2003) 63–72.

[22] P. Krysl and T. Belytschko, An effcient linear-precision partition of unity basis for unstructured meshless methods. *Commun. Numer. Meth. Engng.* **16** (2000) 239–255.

[23] D.Y. Kwak, K.T. Wee and K.S. Chang, An analysis of a broken P_1 -nonconforming finite element method for interface problems. *SIAM J. Numer. Anal.* **48** (2010) 2117–2134.

[24] M. Lai, Z. Li and X. Lin, Fast solvers for 3D Poisson equations involving interfaces in a finite or the infinite domain. *J. Comput. Appl. Math.* **191** (2006) 106–125.

[25] G. Legrain, N. Moës and E. Verron, Stress analysis around crack tips in finite strain problems using the eXtended finite element method. *Int. J. Numer. Meth. Eng.* **63** (2005) 290–314.

[26] D. Leguillon and E. Sanchez-Palencia, *Computation of Singular Solutions in Elliptic Problems and Elasticity*. Wiley (1987).

[27] R.J. LeVeque and Z. Li, The immersed interface method for elliptic equations with discontinuous coefficients and singular sources. *SIAM J. Numer. Anal.* **31** (1994) 1019–1044.

[28] R.J. LeVeque and Z. Li, Immersed interface method for Stokes flowwith elastic boundaries or surface tension. *SIAM J. Sci. Comput.* **18** (1997) 709–735.

[29] T. Lin and X. Zhang, Linear and bilinear immersed finite elements for planar elasticity interface problems. *J. Comput. Appl. Math.* **236** (2012) 4681–4699.

[30] Z. Li, T. Lin and X. Wu, New Cartesian grid methods for interface problems using the finite element formulation. *Numer. Math.* **96** (2003) 61–98.

[31] Z. Li, T. Lin, Y. Lin and R.C. Rogers, An immersed finite element space and its approximation capability. *Numer. Methods Partial Differ. Eq.* **20** (2004) 338–367.

[32] T. Lin, D. Sheen and X. Zhang, A locking-free immersed finite element method for planar elasticity interface problems. *J. Comput. Phys.* **247** (2013) 228–247.

[33] N. Moës, J. Dolbow and T. Belytschko, A finite element method for crack growth without remeshing. *Int. J. Numer. Methods Eng.* **46** (1999) 131–156.

[34] J. Nitsche, Über ein Variationsprinzip zur Lösung von Dirichlet-Problemen bei Verwendung von Teilraumen die keinen Randbedingungen unterworfen sind. *Abh. Math. Sem. Univ. Hamburg* **36** (1971) 9–15.

[35] M. Oevermann, C. Scharfenberg and R. Klein, A sharp interface finite volume method for elliptic equations on Cartesian grids. *J. Comput. Phys.* **228** (2009) 5184–5206.

[36] M.F. Wheeler, An elliptic collocation-finite element method with interior penalties. *SIAM J. Numer. Anal.* **15** (1978) 152–161.